Intermittent dynamics in transient polymer networks under shear: Signs of self-organized criticality

Joris Sprakel,[1,*] Evan Spruijt,[1] Martien A. Cohen Stuart,[1] Matthias A. J. Michels,[2] and Jasper van der Gucht[1]

[1]*Laboratory of Physical Chemistry and Colloid Science, Wageningen University, Dreijenplein 6, 6703 HB Wageningen, The Netherlands*
[2]*Polymer Physics Group, Eindhoven University of TechnologyP. O. Box 513, 5600 MB, Eindhoven, the Netherlands*

In this paper we demonstrate an unusual behavior in the shear-banded flow of a viscoelastic fluid. We report large and patterned fluctuations in the shear stress in an apparently fluid material undergoing steady shear, which we interpret as an intermittent and microscopic fracture and self-healing process. The statistical pattern of the fluctuations is indicative of self-organized criticality, and their magnitude can be directly related to the constitutive instability that underlies the shear banding.

PACS number(s): 47.57.Qk, 05.65.+b, 47.20.Ft

Viscoelastic materials are ubiquitous: both natural, such as the biopolymer networks that constitute the cellular cortex, as well as man made, for example, rheology modifiers found in foods, pharmaceuticals, and coatings. When such materials are deformed at rates faster than they can structurally adapt, part of the structure in the quiescent state is broken down, which in most cases leads to shear thinning. Shear thinning can, when strong enough, make the flow macroscopically unstable, leading to the formation of two, or more, bands of differing shear rate—a phenomenon called shear banding [1,2]. In this paper we discuss the appearance of complex stress fluctuations, with an underlying statistical pattern, in a viscoelastic fluid under steady shear, which we interpret as an intermittent fracture. Healing process taking place around the interface between two shear bands in a viscoelastic fluid under steady deformation. A statistical analysis of these stress fluctuations reveals a pattern that seems to indicate self-organized criticality [3]. Apparently the system spontaneously reaches a nonequilibrium critical point where its dynamics become scale invariant. The magnitude of the stress fluctuations can be directly related to the size of the metastable loop in the constitutive relation underlying the flow instability.

Rheological measurements are carried out under strain rate control on an Anton Paar MCR501 rheometer in a concentric cylinder geometry. The protocols for the velocimetry measurements, with laser Doppler velocimetry, and the rheological protocols are described elsewhere [1]. The material under study is a water-soluble polymer polyethylene oxide (PEO, of 20 kg/mol) with a hydrophobic sticker (an octadecyl alkane) covalently attached to both chain ends (see [1] for preparation procedure). Dissolved in water at sufficient concentration (in this paper at 25 g/L unless stated otherwise), it spontaneously associates into a transient network [4]. The network is composed of self-assembled micellar nodes, with a finite lifetime, interconnected by flexible polymer chains. These systems behave as viscoelastic Maxwell fluids, characterized by a single microscopic relaxation time τ_0 and plateau modulus G_0.

An interesting feature of these systems is that the relaxation time can be tuned with temperature [5] while the plateau modulus is relatively insensitive to temperature (Fig. 1). The relaxation time shows Arrhenius behavior, i.e., decreases exponentially with temperature, which is indicative of a first-order activated process. As stress relaxation primarily occurs through the dissociation of bridged polymer chains between micellar nodes, the activation energy for this process (here $\approx 22 k_B T$) can be interpreted as the energy barrier of bringing a hydrophobic sticker at the chain end of a polymer from its hydrophobic environment in the micellar node to the surrounding aqueous bulk phase. The plateau modulus is a representation of the network topology, i.e., the multiplicity and number of junction points (nodes), and is relatively insensitive to changes in temperature. This allows us to use temperature as a tuning parameter to illustrate the nontrivial scaling of the rheological behavior of these transient networks with relaxation time.

Under steady shear, the tension on the stickers reduces the average lifetime of the polymer bridges, thus disrupting the network structure and producing a severe shear thinning, i.e., a viscosity that decreases strongly with applied shear rate. This makes the flow mechanically unstable [1,6]. The result is that bands of different shear rate are spontaneously formed parallel to the flow direction [Figs. 2(a) and 2(b)]—a phenomenon known as shear banding [1,2]. In the low-shear band the viscosity is high and there are still many junctions, while in the high-shear band many junctions are broken, resulting in a lower viscosity. A stress plateau (see Fig. 3), the
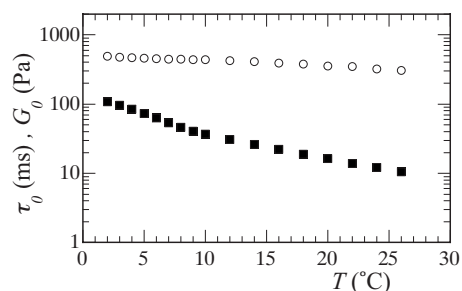

FIG. 1. Zero-shear relaxation time τ_0 ($\square$) and plateau modulus G_0 ($\bullet$) as a function of temperature for a transient associative polymer network at 25 g/L.

*Present address: Dutch Polymer Institute (DPI), P.O. Box 902, 5600 AX Eindhoven, the Netherlands; joris.sprakel@wur.nl
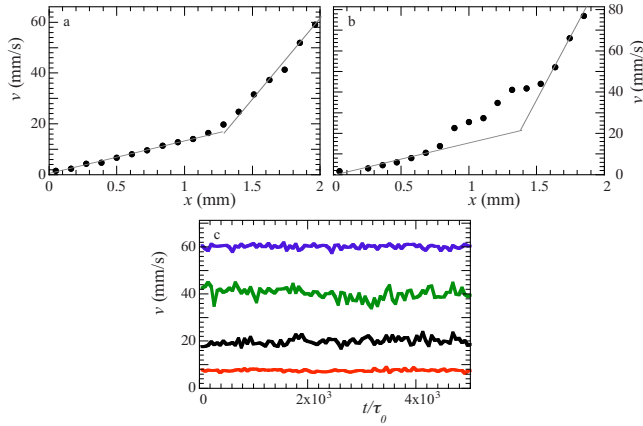
FIG. 2. (Color online) Results from velocimetry measurements: (a) and (b) fluid velocity profiles across the gap (x) of the couette geometry, measured at $T=20$ °C and (a) $\dot{\gamma}\tau_0=0.54$ and (b) 0.74 for a 30 g/L associative polymer solution ($\tau_0=18$ ms); (c) transient velocity measurements ($\dot{\gamma}\tau_0=0.54$) for four positions in the gap; (from top to bottom) (i) near the inner rotating cylinder ($x=1.9$ mm), (ii) and (iii) close to the interface between the shear bands ($x=1.6$ and 1.2 mm, respectively), and (iv) near the stationary outer wall ($x=0.4$ mm) [1].

rheological signature for shear banding, has been observed before for similar telechelic polymers [7], and in a recent paper we showed direct evidence for a shear-banded flow [1]. Such behavior is not unique to this material; it is observed in a wide variety of soft materials, such as solutions of wormlike micelles, colloidal suspensions, and entangled polymer solutions [2]. For our system, this plateau occurs at shear rates $\dot{\gamma}$ on the order of the reciprocal relaxation time τ_0. Velocity profiles measured in this regime. [Figs. 2(a) and 2(b)] indeed show bands of different shear rate. The flow is homogenous at lower shear rates, where the network can easily adjust to the deformation, and at high-shear rates, where the network structure is almost entirely disrupted [1]. A plateau in the stress is associated with a steady state, i.e., when the banding has fully developed. A metastable loop, with a part where the stress is a decreasing function of shear rate, underlies this steady state and can be probed by performing rapid shear rate scans, as we have shown in [1]. These metastable loops were also previously observed by others [6].

When the stress is measured as a function of time at a constant applied shear rate in the shear banding regime, it becomes clear that a true steady state is never reached: the stress keeps undergoing persistent fluctuations (top panel Fig. 4) The magnitude of these stress fluctuations, indicated by the vertical bars in Fig. 3, is on the order of 10 Pa, much larger than the experimental error (<0.1 Pa). Such large fluctuations are only observed in the shear banding regime.

At first glance, the signal may appear to be chaotic. Indeed the stresses display a normal distribution around their average value [Fig. 5(a)] and the power spectrum [Fig. 5(b)] of the raw stress signal shows no dominant frequencies. Chaotic stress responses have been studied in detail for solutions of wormlike micelles [8,9].
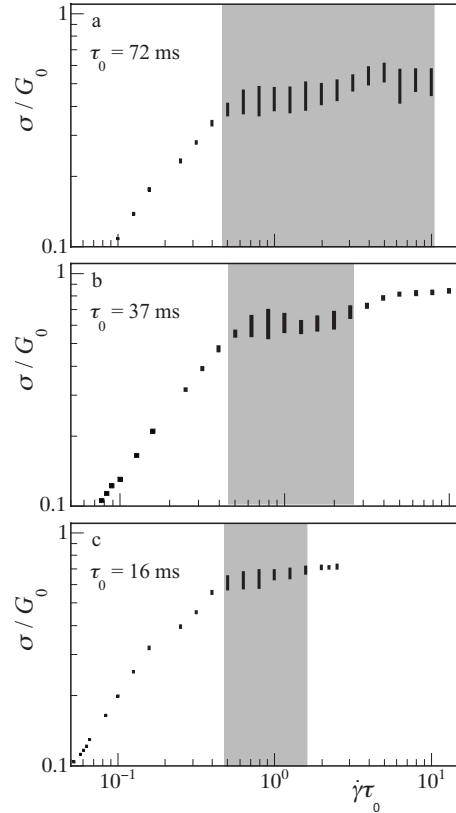
In our case however, a distinct pattern appears when we

FIG. 3. Dimensionless shear stress σ/G_0 versus dimensionless shear rate $\dot{\gamma}\tau_0$ for a transient polymer network at 25 g/L at three different temperatures (and thus three different relaxation times) (a) 5 °C ($\tau_0=72$ ms), (b) 10 °C ($\tau_0=37$ ms), and (c) 20 °C ($\tau_0=16$ ms). The vertical bars indicate the range of stress fluctuations for a given shear rate. The gray region indicates where shear banding and fluctuating stresses are found.

zoom in on the signal (bottom panel Fig. 4). Periods of more or less linear increase in the stress alternate with periods of rapid decrease in the stress. This pattern is reminiscent of the stick-slip motion of two bodies sliding past each other [10]. During a "stick phase" an elastic force builds up, which is spontaneously released by a fracture that propagates between the two bodies, giving rise to a slip motion. After a fracture event, the bodies reconnect to start the stick motion again. A well-known example of stick-slip motion is the movement of tectonic plates in the earth's crust, where intermittent stress drops at the fault lines are responsible for earthquakes [11].

Velocimetry measurements (Fig. 2) in our system showed no slip at either wall; the velocity close to both cylinder walls is constant and equal to the velocity of the wall. In the middle of the gap, however, we do observe significant velocity fluctuations [Fig. 2(c)] [1]. We argue therefore that the intermittent behavior that we observe in the stress response is due to repeated fracture-healing events in the material in the region around the interface between the two shear bands. During a healing stage structure builds up near the interface, which leads to an effective growth of the low-shear band and an increase in the stress. When the stress increases above a certain level, the low-shear band may become unstable, leading to a fracture and a breakdown of the structure that was
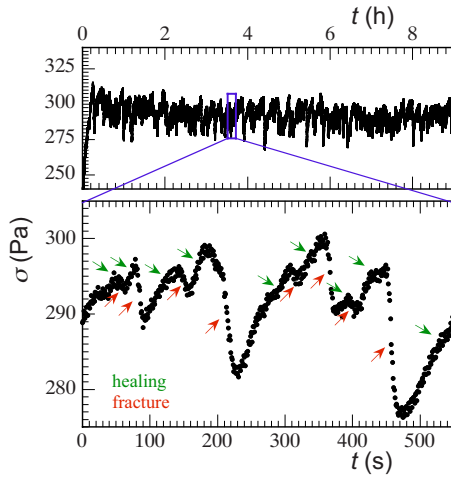
FIG. 4. (Color online) Typical transient stress response in the banded regime, at a steady-shear rate of $\dot\gamma\tau=1$, measured at $T=10$ °C ($\tau_0=36$ ms). Arrows in the bottom panel indicate the two different events constituting the fracture-healing behavior; healing ($\searrow$) and fractures ($\nearrow$). Note that at short time scales $O(\tau_0)$, at the start-up of the shear flow, the stress shows an overshoot, which is not visible here due to the longer sampling interval of 1 s ($\approx 30 \cdot \tau_0$).

built up, with an associated drop in the stress. The repeated growth and shrinkage of the low-shear band leads to the large velocity fluctuations observed in the interfacial region [Fig. 2(c)]. This might also be reflected in the fact that some velocity profiles, often well inside the banded regime, display an irregular region in the center of the gap [Fig. 2(b)], which we previously tentatively interpreted as a "third band" [1].
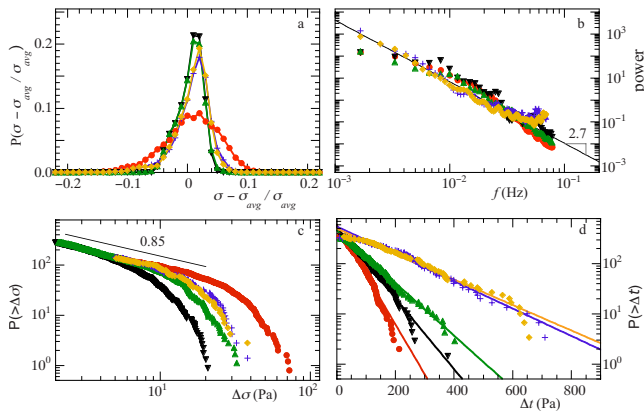

FIG. 5. (Color online) (a) Distributions of the relative fluctuation in stress around their average. (b) Power spectra obtained by Fourier transformation of the raw stress signal. (c) Cumulative distributions of the stress drop $\Delta\sigma$ of fractures. (d) Cumulative distributions of the intervals Δt between fractures; drawn lines are fits to Poisson distributions. All for various shear rates and relaxation times: $\dot\gamma\tau_0=1.0$ and $\tau_0=37$ ms (i.e., $T=10$ °C, ●), $\dot\gamma\tau_0=1.6$ and $\tau_0=37$ ms (▼), $\dot\gamma\tau_0=2.0$ and $\tau_0=37$ ms (▲), $\dot\gamma\tau_0=1.0$ and $\tau_0=96$ ms (i.e., $T=3$ °C, +), and $\dot\gamma\tau_0=1.0$ and $\tau_0=107$ ms (i.e., $T=2$ °C, ◆). Inset in (c) shows the dependence on the decay time τ_i for the interval distribution between fractures as a function of applied shear rate.

Note that the localized and microscopic fractures that we observe should not be confused with the macroscopic fracture observed by Berret and Séréro [12] for fluorocarbon telechelics. In contrast to what we find, these materials do not heal after a microscopic fracture so that the fracture can grow to macroscopic dimensions. This might be due to their much longer microscopic relaxation time, i.e., up to 170 times larger than τ_0 of our material.

While chaos may seem to reign, the dynamics of stick-slip processes are characterized by an underlying statistical pattern [10]. In our case, the cumulative distribution of the total stress drops $\Delta\sigma$ during a fracture [Fig. 5(c)] displays a characteristic power-law behavior, $P(>\Delta\sigma)\propto\Delta\sigma^{-b}$, limited for small $\Delta\sigma$ by experimental noise. The exponent $b=0.85$ we find is close to the value of 0.8 reported for true stick-slip motion [10]. Attempts to explain such scaling behavior often involve the concept of self-organized criticality [3]. According to this theory, driven dissipative dynamical systems spontaneously reach a critical state that is characterized by a power-law distribution of events and power-law behavior in the power spectrum of the fluctuations. Our material obeys the same statistics.

An important aspect in the concept of self-organized criticality is the robustness of the driven-critical state, while critical behavior in equilibrium systems is restricted to a specific combination of the relevant parameters (temperature, pressure, density, etc.). Self-organized critical systems reach the critical state under a broad range of conditions. We find the same robustness: the characteristic power-law behavior in the stress fluctuations is found for a wide range of shear rates and relaxation times (i.e., temperatures) (Fig. 3).

The power-law behavior in the distribution of fracture moments is lost beyond amplitudes of roughly 10 Pa. For larger amplitudes the distribution decays very rapidly. The existence of such a cutoff implies that there is an upper limit to the stress fluctuations, which is obviously related to the bandwidth of the stress fluctuations in Fig. 4.

We find that banding consistently starts at $\dot\gamma\approx0.5\tau_0^{-1}$ and leads to a stress plateau at $\sigma=0.7G_0$, which could suggest that the banding depends trivially on the plateau modulus and relaxation time of these Maxwellian systems. Nonetheless, the magnitude of the stress fluctuations and the shear rate range over which they occur show a nontrivial dependence on relaxation time. By plotting the transient stress response for the same system at the same dimensionless shear rate measured at various temperatures (thus different values of τ_0), we can clearly see that the magnitude ("bandwidth") of the fluctuations increases with increasing τ_0 (Fig. 6). In the same way we observe that the shear rate range over which these intermittent dynamics are found also increases with τ_0 (shaded regions in Fig. 3).

In Fig. 7(b), the difference S between the maximum and minimum stresses, relative to the average stress $\bar\sigma$, is plotted as a function of the microscopic relaxation time. The limits on the stress fluctuations can be explained on the basis of the constitutive relation that underlies the shear banding behavior, which was derived previously [1,6]. The principal ingredient in this mean-field model is that flow enhances dissociation of the junctions. The reason for this is that the shear flow leads to elongation of the bridging chains, resulting in an
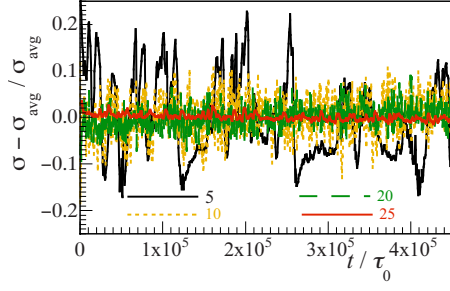
FIG. 6. (Color online) Transient stress responses, plotted as the relative variations in stress around their average value, for four different temperature (indicated in the plot in °C) at $\dot{\gamma}\tau_0 = 1$.

elastic pulling force on the junctions $f \simeq k_B T \tau \dot{\gamma} / \xi$. Here ξ is the typical dimension of a chain in the flow gradient direction (we use $\xi = 2.5$ nm, estimated from the plateau modulus) so that the stretching rate is roughly $\dot{\gamma}\xi$ while the entropic spring constant is $k_B T / \xi^2$. τ is the average lifetime of a junction, i.e., the typical time during which the chains are stretched before they dissociate. The lifetime τ is a function of the shear rate. Assuming that junction dissociation is an activated process, we can write

$$\tau = \tau_0 \exp\left(-\frac{f\delta}{k_B T}\right) = \tau_0 \exp\left(-\frac{\dot{\gamma}\tau\delta}{\xi}\right), \qquad (1)$$

giving an implicit equation for τ in which δ is the length over which the force acts, i.e., the length of the alkyl tail (here
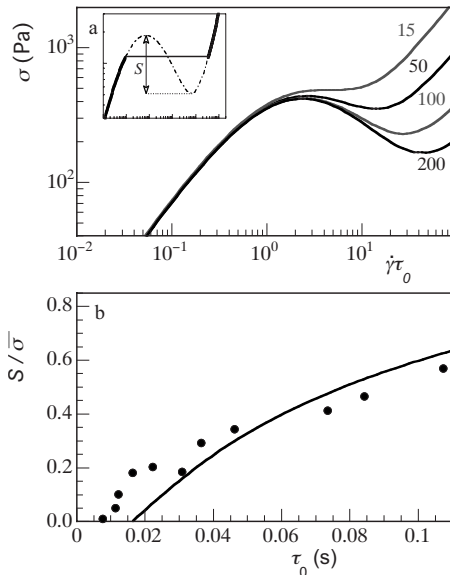

FIG. 7. (a) Flow curves predicted by the microscopic constitutive relation [Eq. (3)] for various relaxation times τ_0 (given in ms). Inset illustrates the metastable loop (dotted line), the steady-state tie line (horizontal plateau), and the definition of the predicted bandwidth S. (b) Experimentally determined bandwidth of the stress fluctuations, given as the difference between maximum and minimum stresses, relative to the average stress $\bar{\sigma}$. Drawn line is the prediction of our model. Note that the loop in the flow curve, and with that the shear banding behavior, disappears for $\tau_0 \lesssim 0.02$ s.

$\delta = 1.8$ nm). We simplify this by expanding the exponential, which gives

$$\tau = \frac{\tau_0}{1 + \delta\dot{\gamma}\tau_0/\xi}. \qquad (2)$$

For small shear rates, $\dot{\gamma}\tau_0 \ll 1$, sticker dissociation is unaffected by the shear rate, $\tau \approx \tau_0$. For high-shear rates, $\dot{\gamma}\tau_0 \gg 1$, the average lifetime is equal to the time it takes to stretch the chain so far that the force becomes $k_B T / \delta$; i.e., $\tau \approx \xi / \delta\dot{\gamma}$.

As derived in [1], the steady-state concentration of bridges can be written as $n_b = nK/(1+K)$, where n is the total concentration of chains (loops and bridges) and $K = k_a / k_d = k_a \tau$, with k_a and k_d as the association and dissociation rates, respectively. We assume that the equilibrium constant K_0 in rest is constant when τ_0 is varied ($k_a = K_0 / \tau_0$), with $K_0 = 0.1$ found from the experimentally determined ratio of bridges to loops (results not shown). The shear stress is determined by the number of active bridges and the average force per bridge, which both depend on the shear rate as follows:

$$\sigma = \xi n_b f + \eta_{\text{eff}}\dot{\gamma} = \dot{\gamma}\left(\frac{k_a n \tau^2 k_B T}{1 + k_a \tau}\right) + \eta_{\text{eff}}\dot{\gamma}, \qquad (3)$$

with η_{eff} as the high-shear viscosity, corresponding to the disrupted network (here $\eta_{\text{eff}} \approx 0.5$ Pa s) and τ is given by Eq. (2). Note that Eq. (3) is not frame invariant. In Fig. 3(a), this equation is plotted together with the experimental flow curve. The model predicts a nonmonotonic stress-shear rate relation.

The decreasing part of this curve is mechanically unstable and corresponds to the regime where the shear banding and the stress fluctuations are observed. Clearly, no matter how the two shear bands arrange themselves, the stress in this region is bounded by the maximum and the minimum in the stress-shear rate curve. Our microscopic model predicts that the loop becomes more pronounced if the microscopic relaxation time τ_0 increases [Fig. 7(a)], which is in good agreement with the experimentally observed bandwidths of the stress fluctuations [Fig. 7(b)].

The fact that the stress fluctuations are bounded by the metastability in the constitutive relation is analogous to the limitations on critical density fluctuations in equilibrium systems, which are bounded by the metastable van der Waals–loop in the governing thermodynamic potential.

The "quiescent" intervals between two fracture events show exponential (Poisson) distributions [Fig. 5(d)] and display a cutoff at long interval times that is related to the cutoff in fracture magnitudes discussed above. The Poisson behavior implies that the intermittent fracture events occurring at different times are not correlated; in other words there is no memory of past fracture events. The reason for this lack of memory could be that the material quickly "heals" once a fracture is terminated since the microscopic relaxation time of the material is between 30 and 100 ms in this study, much shorter than the typical time between fracture events.

The average interval time τ_i between two fracture events is on the order of 10–100 s. This is roughly a thousand times longer than the microscopic relaxation time of the material,
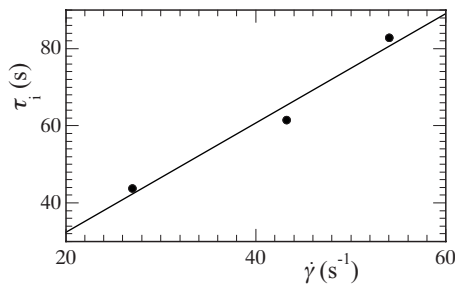
FIG. 8. Characteristic time interval τ_i between fracture events as a function of overall applied shear rate, from fitting a single exponential decay to the data shown in Fig. 5(d), for $T=10\,°$C ($\tau_0 = 37$ ms).

suggesting that the stress buildup is a process that involves the creation of many junctions. As seen in Fig. 5(d), an increase in the microscopic relaxation time (from 36 to 107 ms) leads to an increase in τ_i (from 40 to 170 s). When the formation of single connections is slowed down, the collective buildup process will also be slower. More counterintuitive is the observation that τ_i increases linearly with the applied shear rate (Fig. 8), while the dynamics of most processes are enhanced when the shear rate, and with that the energy input into the system, is increased. The scenario that we propose is that the formation of new connections (association) across the gap is hindered by the velocity gradient between two neighboring fluid elements, as the average contact time between two nodes decreases.

In this paper we have presented observations of intermittently patterned stress fluctuations in the steady-shear flow of an apparently simple viscoelastic fluid. We hypothesize that these are related to an indefinitely repeating microscopic fracture and a self-healing behavior inside the liquid. This seems to be consistent with previous interpretations of chaotic stress fluctuations in shear-banded materials as interfacial instabilities [9,13]. Here we have shown however that, while appearing chaotic at first sight, these fluctuations are characterized by an underlying statistical pattern, which is indicative of self-organized criticality. In analogy with critical fluctuations in equilibrium systems, we have shown that the stress fluctuations accompanying this nonequilibrium critical state are bounded by the metastable loop in the constitutive relation that underlies the shear banding. This opens up new possibilities as concepts known from the study of equilibrium critical phenomena now can be employed to understand these nonequilibrium phase transitions.

[1] J. Sprakel, E. Spruijt, M. A. Cohen Stuart, N. A. M. Besseling, M. P. Lettinga, and J. van der Gucht, Soft Matter **4**, 1696 (2008).

[2] P. Olmsted, Rheol. Acta **47**, 283 (2008).

[3] P. Bak, C. Tang, and K. Wiesenfeld, Phys. Rev. Lett. **59**, 381 (1987).

[4] Y. Séréro, R. Aznar, G. Porte, J. F. Berret, D. Calvet, A. Collet, and M. Viguier, Phys. Rev. Lett. **81**, 5584 (1998).

[5] T. Annable, R. Buscall, R. Ettelaie, and D. Whittlestone, J. Rheol. **37**, 695 (1993).

[6] E. Michel, J. Appell, F. Molino, J. Kieffer, and G. Porte, J. Rheol. **45**, 1465 (2001).

[7] J.-F. Le Meins and J.-F. Tassin, Macromolecules **34**, 2641 (2001).

[8] R. Ganapathy and A. K. Sood, Phys. Rev. Lett. **96**, 108301 (2006).

[9] S. M. Fielding, Soft Matter **3**, 1262 (2007).

[10] Hans Jacob S. Feder and J. Feder, Phys. Rev. Lett. **66**, 2669 (1991).

[11] W. F. Brace and J. D. Byerlee, Science **153**, 990 (1966).

[12] J.-F. Berret and Y. Séréro, Phys. Rev. Lett. **87**, 048303 (2001).

[13] M. D. Eggert and S. Kumar, J. Colloid Interface Sci. **278**, 234 (2004).